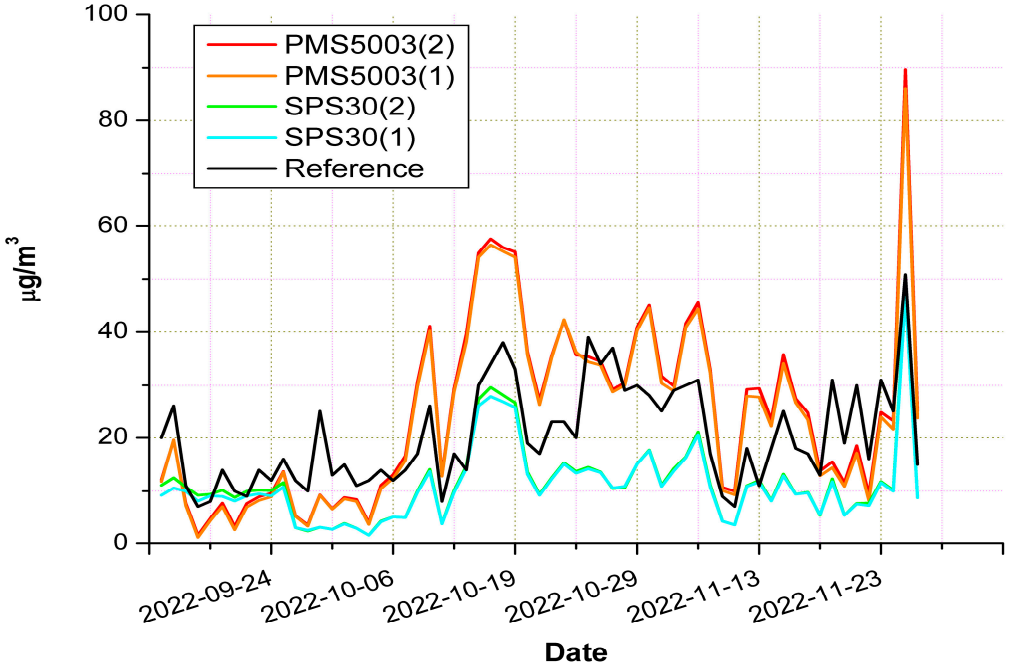

Figure 5. Time series of sensors under evaluation compared with the reference device.

As for the consistency, or variability, both the models showed a good performance, and, as also underlined by the time-series plots, substantial agreement between the two copies of the same models can be observed in Table 3, which highlights the high correlation between them. As a matter of fact, all the values reported in this table are very close to 1, indicating very good intra-model consistency.

Table 3. Coefficient of correlations related to the sensors involved in the experiment.

	PMS5003(2)	PMS5003(1)	SPS30(2)	SPS30(1)
PMS5003(2)	1.000	0.999	0.790	0.819
PMS5003(1)	0.999	1.000	0.785	0.813
SPS30(2)	0.790	0.785	1.000	0.997
SPS30(1)	0.819	0.813	0.997	1.000

The ability of each sensor to reflect the reference measurements could also be evaluated by examining the plots presented in Figure 6. They show that the PMS5003 model correlated slightly better with the reference device than the SPS30 sensors. As a matter of fact, the R^2 was 0.61 for both copies of the PMS5003 model, while the SPS30 sensors had an R^2 equal to 0.57 and 0.55. The slope of the linear fit line computed for the two models explained both the tendency of the PMS5003 model to overestimate the PM_{10} concentrations and the fact that the SPS30 model tended to underestimate them. The plots in Figure 6 show that the slope of the PMS5003 model was roughly threefold the slope of the SPS30 sensors; however, the most important aspect is represented by the position of the linear fit line, which lies over the 1:1 reference line in the case of the PMS5003 model, and underneath it in the case of the SPS30 model. It is useful to recall that the slopes of linear fit lines close to unity and bias values near 0 denote the good performance of the device under evaluation. From Figure 6, it can also be noted that the values related to the slope and bias were very similar for the two copies of the same models. This finding, in conjunction with the values reported for the intra-model correlation, confirmed the consistency of both LCS models.

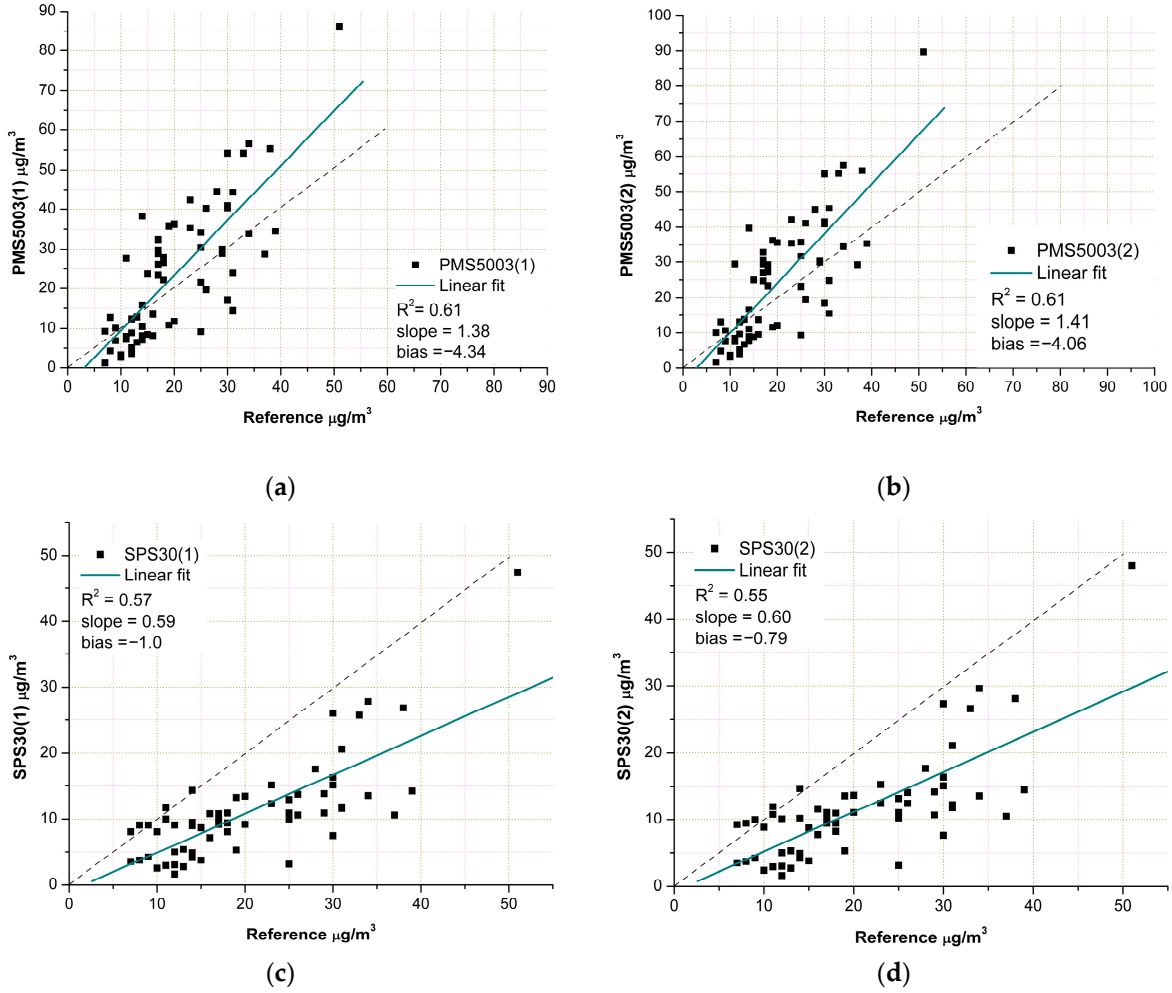

Figure 6. (**a**) PMS5003(1); (**b**) PMS5003(2); (**c**) SPS30(1); (**d**) SPS30(2). Comparison between the four copies of the PM sensors involved in this research and the reference device. The solid line represents a linear regression fit computed through the ordinary least squares method, while the dashed line indicates the 1:1 reference line. In the corners of the figures, the statistics are reported. The slope and bias are related to the slope and the intercept of the linear fit.

The complete overview of the sensor performance is provided in Table 4, where the values of the R^2, MAE, RMSE, MNB, and CV indicators are presented. Concerning R^2, MAE, and RMSE, the performance of the two models was quite similar, while a substantial difference was observed only in the MNB values. A possible explanation for this difference can be found by analyzing Figure 6. In the plots of this figure, one can note that both the linear fit lines of the PMS5003 model are very close to the 1:1 reference line, or rather, there is an intersection around the 10 µg/m^3 concentration level. On the contrary, in the case of the SPS30 model, the fit lines lie underneath the reference line in a more distant position.

Table 4. Performance indicators of each copy of the sensors in relation to the reference measurements. The MNB and CV values are in relation to the two sensor models considered in this research.

Sensor	R^2	MAE	RMSE	Slope	Bias	MNB	CV
PMS5003(2)	0.61	9.56	12.09	1.41	−4.06	0.14	1.96%
PMS5003(1)	0.61	9.3	11.63	1.38	−4.34		
SPS30(2)	0.55	9.19	11.02	0.60	−0.79	−0.44	2.76%
SPS30(1)	0.57	9.47	11.26	0.59	−1.0		

5.2. Results after Applying the Correction Factor for the Humidity Effects

As explained earlier, an algorithm to correct the negative effect of humidity was applied to the sensor measurements to evaluate potential improvements in their performance. For this reason, the relative humidity (RH) was measured and logged along with the other sensor data to compose the final dataset. Figure 7 shows the levels of relative humidity registered during the period of the experiment.

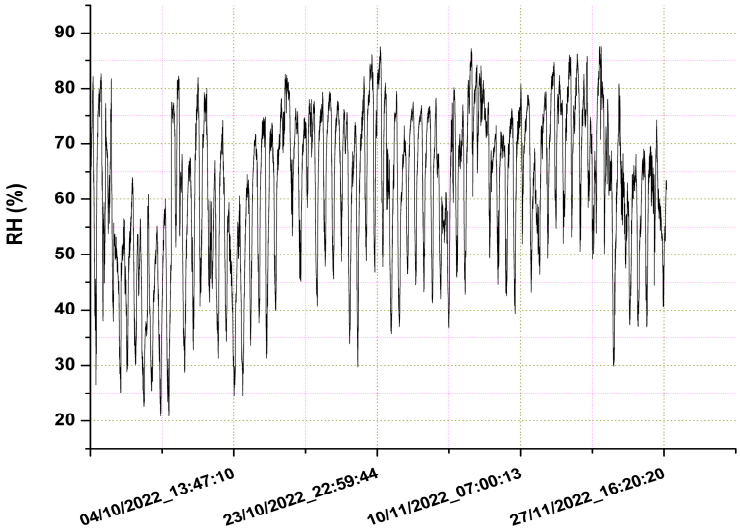

Figure 7. Time series of the relative humidity registered during the experiment.

The RH values were used to compute the corrected measurements of the sensors as indicated in Equations (6) and (7). Once we had performed the correction, the daily averages were subsequently calculated for comparison with the reference data. From Figure 7, it can be noted that the range of RH values was between 22% and 88%. This finding gave us an idea of the variability in the conditions during the experimental period in terms of humidity levels, while the average was equal to 62%.

Table 5 summarizes the performance indicators of the sensors considering the humidity effect and compares them with their uncorrected measurements to quantify the effectiveness of the correction algorithm.

Table 5. The performance indicators of the sensors under evaluation. The rows indicating PMS5003(1), PMS5003(2), and so on, show the data related to the uncorrected measurements, while the labels k = 0.5 and k = 0.62 indicate the data calculated by setting k = 0.5 and k = 0.62 in Equation (7). Data reported in bold characters denote the best performance.

Sensor	R^2	MAE	RMSE	Slope	Bias
PMS5003(2)	0.61	9.56	12.09	1.41	−4.06
PMS5003(2) (k = 0.5)	**0.65**	**6.59**	**8.24**	**0.81**	**−11.48**
PMS5003(2) (k = 0.62)	0.65	7.21	8.84	0.74	−12.62
PMS5003(1)	0.61	9.3	11.63	1.38	−4.34
PMS5003(1) (k = 0.5)	0.65	6.81	8.5	0.75	−12.59
PMS5003(1) (k = 0.62)	0.65	7.21	8.84	0.81	−11.48
SPS30(2)	0.55	9.19	11.02	0.60	−0.79

Table 5. *Cont.*

Sensor	R^2	MAE	RMSE	Slope	Bias
SPS30(2) (k = 0.5)	0.50	13.31	15.03	1.42	−7.23
SPS30(2) (k = 0.62)	0.48	13.85	15.6	1.52	−6.81
SPS30(1)	**0.57**	**9.47**	**11.26**	**0.59**	**−1.0**
SPS30(1) (k = 0.5)	0.52	13.56	15.24	1.50	−6.72
SPS30(1) (k = 0.62)	0.51	14.1	15.8	1.62	−6.28

The data summarized in the above table reflect the trends of the sensor measurements, which are more extensively illustrated in Figure 8.

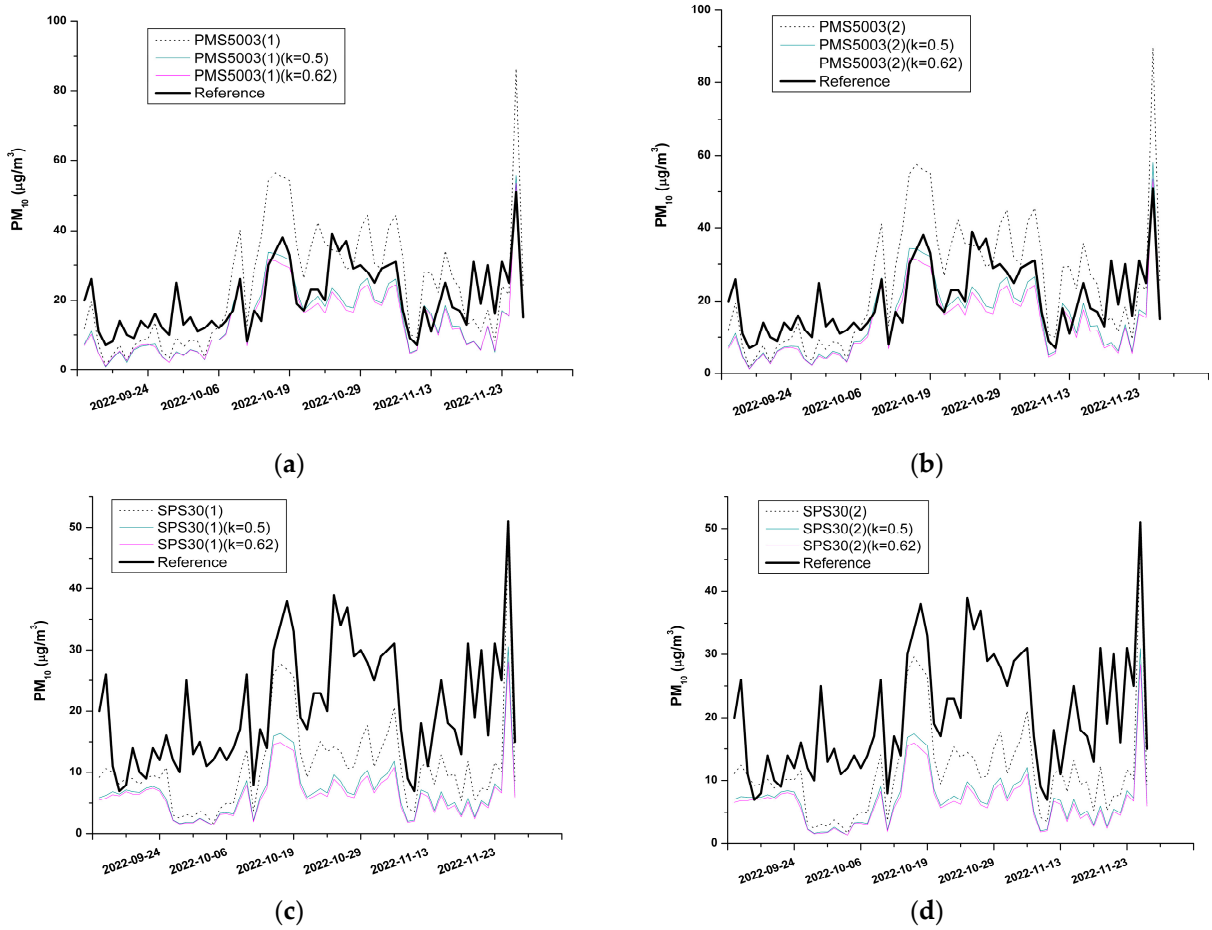

Figure 8. (**a**) PMS5003(1); (**b**) PMS5003(2); (**c**) SPS30(1); (**d**) SPS30(2). Time series of the sensor measurements compared with the reference device (thick black line). The dotted line is relative to the sensor data without the application of Equations (6) and (7). The straight thinner lines indicate the sensor measurements after applying the correction to include the humidity effect. The labels k = 0.5 and k = 0.62 indicate the different values of the "k" parameter in Equation (7).

The analysis of the data presented in Table 5 showed that the corrective formulas to include the humidity effects produced an improvement in the performance of the PMS5003 sensor model. This finding was corroborated by the increase of R^2 values, and the decrease of MAE and RMSE values with respect to the case of the uncorrected sensor measurements (denoted in the table as PMS5003(2) and PMS5003(1)). This phenomenon characterized both copies of the PMS5003 model (PMS5003(2) and PMS5003(1)), even

though the PMS5003(2) model corrected using the 0.5 value for the "k" parameter showed a slightly better performance compared with the other cases.

Table 5 also reports that, in the case of the SPS30 model, the corrective algorithm could not provide an improvement for both copies of the sensor. The decrease in R^2 values, the increase in MAE and RMSE, and the widening of the gap between the slope parameter and the unity value indicated the worsening of their performance.

To understand the reasons for the different outcomes after applying the correction to the two sensor models under evaluation, it is necessary to consider that the effect of the humidity was the hygroscopic growth of the aerosol particles due to the condensation of water vapor. This phenomenon led to an overestimation of the PM concentration by the sensors, which could not distinguish the real dimensions of the particles. To counterbalance this effect, the concentration read by the sensor was divided by the "C" factor (see Equation (6)), which is linked to the ambient relative humidity: the greater the RH value, the higher the value of the "C" factor is. As can be seen in Figures 5, 6 and 8, the uncorrected measurements of the PMS5003 sensors tended to overestimate the real PM concentration provided by the reference; thus, the application of the Equations (6) and (7) decreased the values of the readings performed by these sensors, making them closer to the real PM concentrations. On the contrary, the uncorrected measurements of the SPS30 model underestimated the real PM concentrations (see Figures 5, 6 and 8); therefore, the application of the correction factor contributed to further lowering the value of the sensor readings, causing a widening of the gap between the real concentration levels and those provided by the sensors.

6. Discussion

6.1. Analysis of Results

The results concerning the performance of the models evaluated in this study can be better understood by comparing them with the data found in previous, similar works. We mentioned earlier that a comparison with several existing studies was not an easy task due to the different conditions surrounding the various experiments and the different metrics used for assessing the LCM/LCS performance. Nevertheless, we selected two such studies with very similar characteristics to the present experiment.

In their research, Vogt and Castell [23] performed an on-field evaluation of three LCM models. Two of the devices under evaluation were the Ensense and the Airly LCM model, commercially available at the current date. The operation of the Ensense model is based on the PMS5003 sensor, while the Airly monitor uses an SPS30 sensor. The duration of their research (53 days) was shorter than the one of the experiment described in the present study, but similar to it. They assessed the performance of the LCMs using gravimetric and optical reference instrumentations and by considering the hourly and daily averages of the measurements. In Table 6, the results related to the sensors involved in the present study are compared with the results from Vogt and Castell's study by considering only the daily averages.

In the same table, the performance indicators determined by the AQ-SPEC program [18] are presented for comparison with this research. In this work, a notable number of LCMs and LCSs were evaluated on-field using both optical and beta-attenuator reference instrumentations. The assessment of the devices was performed by considering 5 min, hourly, and daily averages; however, in accordance with the present study, only the results related to the daily averages are summarized. Another element in common with the present work characterizing the AQ-SPEC program was the duration of the LCS/LCM tests, which was roughly equal to two months for each device under evaluation.

By inspecting the table above, one can note a marked heterogeneity in the values of almost all the indicators related to the same sensor model. The reasons for these wide ranges are ascribed to various factors, mainly, different reference types, and PM concentration ranges used in the evaluations. The table also shows that data completeness could be found only for the R^2, slope, and bias parameters.

Table 6. A summary of the performance indicators determined in this work and previous studies related to LCMs using the SPS30 and PMS5003 sensors. Data refer to the PM_{10} concentration measurements. The ranges of the indicators express the minimum and maximum values found, considering that, in the same study, several copies of the same model were evaluated using different types of reference devices.

LCS Model	LCM Model	R^2	RMSE	MAE	CV	Slope	Bias	Reference
PMS5003	SentinAir	0.61	11.63–12.09	9.3–9.56	1.96%	1.38–1.41	−4.06/−4.34	This study
PMS5003	Airly	0.27–0.47	20.5–21.4	16.4–17.8	1.3%	1.17–1.24	−23.4/−46.3	AQ-SPEC [18]
PMS5003	Airly	0.71–0.89	3.79–11.29	-	-	0.64–0.7	−0.11/−1.61	Castell [23]
PMS5003	Airquality Egg 2022	0.27–0.62	23.1–24.9	16.3–18.6	4.2%	1.01–1.72	−24.6/−29.14	AQ-SPEC [18]
PMS5003	PurpleAir PA-II	0.68–0.74	-	-	≅ 0%	1.21–1.70	−0.6/−20.2	AQ-SPEC [18]
PMS5003	Redspira	0.35–0.52	31.2–35.3	28–32.6	5.8%	1.02–1.37	−37.1/−41.4	AQ-SPEC [18]
PMS5003	Smart citizen kit II	0.10–0.17	-	-	6%	2.61–3.05	−157.0/−198.6	AQ-SPEC [18]
PMS5003	Lunar outpost	0.06–0.08	-	-	4.3%	2.63–3.38	−124.3/−140.9	AQ-SPEC [18]
SPS30	Ensense	0.9	1.92–2.26	-	z-	0.26–0.32	−9.39/−9.79	Castell [23]
SPS30	TSI Bluesky	0.28–0.34	-	-	11%	0.33–0.53	−4.5/−11.6	AQ-SPEC [18]
SPS30	Atmotube Pro	0.31–0.39	-	-	5.6%	0.83–0.98	−17.0/−31.4	AQ-SPEC [18]
SPS30	-	0.18–0.30	-	-	2.4%	0.77–1.61	−18.3/−19.9	AQ-SPEC [18]
SPS30	SentinAir	0.55–0.57	9.19–9.47	11.02–11.26	2.76%	0.59–0.60	−0.79/−1.0	This study

If we consider the LCMs using the SPS30 sensor separately from those employing the PMS5003 model, we can see that the ranges of R^2 were 0.18–0.9, and 0.06–0.89, respectively. Therefore, the values found in this work for PMS5003 (R^2 = 0.61) and SPS30 (R^2 = 0.55–0.57) indicate better performance in relation to the median value of R^2 found by the previous studies (R^2 = 0.41 for PMS5003 and R^2 = 0.36 for SPS30).

Table 6 also indicates that the ranges of the RMSE for SPS30 and PMS5003 were, respectively, 1.92–9.47 μg/m^3 and 3.79–35.3 μg/m^3. If we compare these ranges with the data found in this experiment (RMSE = 9.19–9.47 μg/m^3 for SPS30, RMSE = 11.63–12.09 μg/m^3 for PMS5003), we can note that the SPS30 displayed a worse performance, even though it has to be said that there was just one record in the table to compare it with; meanwhile, in the case of the other sensor model, the RMSE values were placed in the middle of the range found by the previous studies.

The other indicator presenting a completeness of data was the slope of the linear fit (see also Figure 6). As shown in Table 6, the ranges were equal to 0.26–1.61 for the SPS30 model and 0.64–3.38 for the PMS5003 model. In this regard, by considering that the ranges found in this study were, respectively, 0.59–0.60 and 1.38–1.41 for the SPS30 and PMS5003 models, we could conclude that the SPS30 model evaluated in this study showed lower slopes with respect to the overall median value (equal to 0.93), while the PMS5003 model was characterized by slopes more in line with the overall median value (equal to 1.37).

The coefficient of variation (CV) is the indicator that provides quantitative information about the consistency of the sensors or devices belonging to the same model. The values found by this work (1.96% for PMS5003 and 2.76% for SPS30) were much lower than the maximum CV found by the previous study (equal to 5.8% for PMS5003 and 11% for SPS30).

Unfortunately, we could not find MAE values for the SPS30 sensor in any previous works, but in the case of the PMS5003 model, they ranged from 9.3 μg/m^3 to 32.6 μg/m^3. Thus, the PMS5003 model evaluated in this study showed a better performance in terms of MAE values.

As shown in Tables 1 and 4, the PMS5003 model featured an MNB of 0.14 and a CV of 1.96%, which fall in the range of the values characterizing Tier III. Thus, according

to the classification proposed by the EPA guidelines, this sensor model can be used for supplemental monitoring to complete the data provided by the regulatory monitoring network and achieve a better spatio-temporal resolution for pollutant maps. In the case of the SPS30 model, we found that it presented an MNB of 0.44 and a CV of 2.76%, which assigned this model to Tier I. The possible uses of this sensor model are therefore related to the informal indication of pollutant presence.

6.2. EPA Guidelines Limits

The guidelines proposed by the EPA offer a practical tool that is useful for supporting the understanding of the most appropriate use, or application area, of an LCS or LCM, especially considering that the performance indicators related to the same sensor can present a wide range of values, as can be found in Table 6. The algorithm responsible for the "tier" selection proposed in the guidelines is based on the computation of the MNB and the CV. The first parameter takes into account the measurement discrepancies between the device under evaluation and the reference, while the CV provides a quantification of the consistency of the devices. Both these parameters are expressed by non-dimensional values, preserving the generality of the guidelines.

However, it can also be noted that the decision process for the selection of the different "tiers" lacks an indicator through which the grade of the correlation of the device with the reference is taken into account. This suggests that the addition of such an indicator to the mechanism at the basis of the tier selection could improve the effectiveness of the guidelines. The most suitable candidates could be the R^2 and the slope of the linear fit line, because they are both non-dimensional parameters.

Nevertheless, a more detailed analysis of these indicators showed that the coefficient of determination (R^2) depends on the range of reference measurements and the duration of the on-field evaluation. In particular, the wider the range of the pollutant concentration values registered by the reference device, the higher the probability of obtaining R^2 values close to unity [11] is. This suggests that the selection of the slope of the linear fit line (see Figure 6) could be an additional indicator to use together with the MNB and the CV for "tiers" determination, but such a decision must be corroborated by targeted, detailed studies, which was beyond the limits of this work. Another limit of this research was the number of LCSs evaluated, the type of reference device considered, and the temporal frequency of the records comprising the measurement database (e.g., 5min, daily, or hourly averages). More specifically, this preliminary investigation performed an evaluation on the basis of daily averages but did not clarify if the application area ("tier") of the evaluated sensors may be assigned to different "tiers" by changing the temporal average of the measurements (e.g., by considering hourly averages) or by changing the reference type.

7. Conclusions

The EPA guidelines offer a useful tool for assessing the most suitable application area, or use, of an LCS/LCM for air quality monitoring. To the best of our knowledge, until now, the performance of the PM sensor models considered in this work had not been analyzed in light of the EPA guidelines by other studies. Therefore, the SPS30 sensor produced by Sensirion and the PMS5003 sensor produced by Plantower were tested in this study using the SentinAir device as a LCM. Their performance in measuring PM_{10} concentrations was evaluated through an on-field test using a gravimetric reference providing daily averages of PM_{10}.

We found that including the effects of the humidity by applying a correction algorithm proposed in previous works could improve the performance of the PMS5003 sensor models. We also found that, as prescribed by the guidelines, considering the MNB and CV indicators, the PMS5003 sensor could be used for supplementing regulatory monitoring networks, while the SPS30 sensor could be used to provide informal information about the presence of pollutants. However, even though the EPA guidelines represent without a doubt an efficient tool to guide the user through the jungle of the low-cost devices for air quality

monitoring available on the market, we found that some improvements to the selection criteria characterizing the guidelines are necessary.

In our opinion, adding an indicator that takes into account the grade of correlation between the reference and the device under evaluation could make the guidelines more efficient in providing indications about the most appropriate application area. However, a rigorous analysis to confirm this aspect could represent a matter for future studies.

Author Contributions: Conceptualization, D.S.; methodology, D.S.; software, D.S.; validation, D.S.; formal analysis, D.S.; investigation, D.S.; resources, M.P.; data curation, D.S.; writing—original draft preparation, D.S.; writing—review and editing, D.S.; visualization, D.S.; supervision, D.S. All authors have read and agreed to the published version of the manuscript.

Funding: This research received no external funding.

Institutional Review Board Statement: Not applicable.

Informed Consent Statement: Not applicable.

Data Availability Statement: Data are available by contacting the author at domenico.suriano@enea.it.

Conflicts of Interest: The authors declare no conflict of interest.

References

1. Kheirbek, I.; Wheeler, K.; Walters, S.; Kass, D.; Matte, T. $PM_{2.5}$ and ozone health impacts and disparities in New York City: Sensitivity to spatial and temporal resolution. *Air Qual. Atmos. Health* **2013**, *6*, 473–486. [CrossRef] [PubMed]
2. Yorifuji, T.; Bae, S.; Kashima, S.; Tsuda, T.; Doi, H.; Honda, Y.; Kim, H.; Hong, Y.C. Health impact assessment of PM_{10} and $PM_{2.5}$ in 27 Southeast and East Asian cities. *J. Occup. Environ. Med.* **2015**, *57*, 751–756. [CrossRef]
3. Makri, A.; Stilianakis, N.I. Vulnerability to air pollution health effects. *Int. J. Hyg. Environ. Health* **2018**, *211*, 326–336. [CrossRef] [PubMed]
4. Pope, C.A., III; Dockery, D.W. Health Effects of Fine Particulate Air Pollution: Lines that Connect. *J. Air Waste Manag. Assoc.* **2006**, *56*, 709–742. [CrossRef] [PubMed]
5. Zhao, A.; Bollasina, M.A.; Crippa, M.; Stevenson, D.S. Significant climate impacts of aerosol changes driven by growth in energy use and advances in emission control technology. *Atmos. Chem. Phys.* **2019**, *19*, 14517–14533. [CrossRef]
6. Velasco, A.; Ferrero, R.; Gandino, F.; Montrucchio, B.; Rebaudengo, M. A mobile and low-cost system for environmental monitoring: A case study. *Sensors* **2016**, *16*, 710. [CrossRef]
7. Mooney, D. *A Guide for Local Authorities Purchasing Air Quality Monitoring Equipment*; Technical Report; AEA Technology Plc: Harwell, UK, 2006.
8. Kularatna, N.; Sudantha, B.H. An environmental air pollution monitoring system based on the IEEE 1451 standard for low cost requirements. *IEEE Sens. J.* **2008**, *8*, 415–422. [CrossRef]
9. Castell, N.; Dauge, F.R.; Schneider, P.; Vogt, M.; Lerner, U.; Fishbain, B.; Broday, D.; Bartonova, A. Can commercial low-cost sensor platforms contribute to air quality monitoring and exposure estimates? *Environ. Int.* **2017**, *99*, 293–302. [CrossRef]
10. Kumar, P.; Morawska, L.; Martani, C.; Biskos, G.; Neophytou, M.; Di Sabatino, S.; Bell, M.; Norford, L.; Britter, R. The rise of low-cost sensing for managing air pollution in cities. *Environ. Int.* **2015**, *75*, 199–205. [CrossRef]
11. Karagulian, F.; Barbiere, M.; Kotsev, A.; Spinelle, L.; Gerboles, M.; Lagler, F.; Redon, N.; Crunaire, S.; Borowiak, A. Review of the Performance of Low-Cost Sensors for Air Quality Monitoring. *Atmosphere* **2019**, *10*, 506. [CrossRef]
12. Snyder, E.G.; Watkins, T.H.; Solomon, P.A.; Thoma, E.D.; Williams, R.W.; Hagler, G.S.; Shelow, D.; Hindin, D.A.; Kilaru, V.J.; Preuss, P.W. The Changing Paradigm of Air Pollution Monitoring. *Environ. Sci. Technol.* **2013**, *47*, 11369–11377. [CrossRef] [PubMed]
13. Kang, Y.; Aye, L.; Ngo, T.D.; Zhou, J. Performance evaluation of low-cost air quality sensors: A review. *Sci. Total Environ.* **2022**, *818*, 151769. [CrossRef] [PubMed]
14. Guidi, V.; Carotta, M.C.; Fabbri, B.; Gherardi, S.; Giberti, A.; Malagù, C. Array of sensors for detection of gaseous malodors in organic decomposition products. *Sens. Actuators B Chem.* **2012**, *174*, 349–354. [CrossRef]
15. Suriano, D.; Rossi, R.; Alvisi, M.; Cassano, G.; Pfister, V.; Penza, M.; Trizio, L.; Brattoli, M.; Amodio, M.; De Gennaro, G. A Portable Sensor System for Air Pollution Monitoring and Malodours Olfactometric Control. In *Sensors and Microsystems: AISEM 2011 Proceedings*; Lecture Notes in Electrical Engineering; Springer: Boston, MA, USA, 2012; Volume 109. [CrossRef]
16. Cavaliere, A.; Carotenuto, F.; Di Gennaro, F.; Gioli, B.; Gualtieri, G.; Martelli, F.; Matese, A.; Toscano, P.; Vagnoli, C.; Zaldei, A. Development of Low-Cost Air Quality Stations for Next Generation Monitoring Networks: Calibration and Validation of $PM_{2.5}$ and PM_{10} Sensors. *Sensors* **2018**, *18*, 2843. [CrossRef] [PubMed]
17. Lewis, A.; Edwards, P. Validate personal air-pollution sensors. *Nature* **2016**, *535*, 29–31. [CrossRef]

18. AQ-SPEC; South Coast Air Quality Management District. South Coast Air Quality Management District Air Quality Sensor Performance Evaluation Reports. Available online: http://www.aqmd.gov/aq-spec/evaluations#&MainContent_C001_Col00=2 (accessed on 9 February 2023).
19. Williams, R.; Kilaru, V.; Snyder, E.; Kaufman, A.; Dye, T.; Rutter, A.; Russell, A.; Hafner, H. *Air Sensor Guidebook*; US Environmental Protection Agency: Washington, DC, USA, 2014.
20. Trizio, L.; Brattoli, M.; De Gennaro, G.; Suriano, D.; Rossi, R.; Alvisi, M.; Cassano, G.; Pfister, V.; Penza, M. Application of artificial neural networks to a gas sensor-array database for environmental monitoring. In *Sensors and Microsystems*; Springer: Boston, MA, USA, 2012; pp. 139–144. [CrossRef]
21. Suriano, D.; Penza, M. Assessment of the Performance of a Low-Cost Air Quality Monitor in an Indoor Environment through Different Calibration Models. *Atmosphere* **2022**, *13*, 567. [CrossRef]
22. Gao, M.; Cao, J.; Seto, E. A distributed network of low-cost continuous reading sensors to measure spatiotemporal variations of $PM_{2.5}$ in Xi'an, China. *Environ. Pollut.* **2015**, *199*, 56–65. [CrossRef]
23. Vogt, M.; Schneider, P.; Castell, N.; Hamer, P. Assessment of Low-Cost Particulate Matter Sensor Systems against Optical and Gravimetric Methods in a Field Co-Location in Norway. *Atmosphere* **2021**, *12*, 961. [CrossRef]
24. Kosmopoulos, G.; Salamalikis, V.; Pandis, S.N.; Yannopoulos, P.; Bloutsos, A.A.; Kazantzidis, A. Low-cost sensors for measuring airborne particulate matter: Field evaluation and calibration at a South-Eastern European site. *Sci. Total Environ.* **2020**, *748*, 141396. [CrossRef]
25. Masic, A.; Bibic, D.; Pikula, B.; Blazevic, A.; Huremovic, J.; Zero, S. Evaluation of optical particulate matter sensors under realistic conditions of strong and mild urban pollution. *Atmos. Meas. Tech.* **2020**, *13*, 6427–6443. [CrossRef]
26. Han, I.; Symanski, E.; Stock, T.H. Feasibility of using low-cost portable particle monitors for measurement of fine and coarse particulate matter in urban ambient air. *J. Air Waste Manag. Assoc.* **2017**, *67*, 330–340. [CrossRef]
27. Jovašević-Stojanović, M.; Bartonova, A.; Topalović, D.; Lazović, I.; Pokrić, B.; Ristovski, Z. On the use of small and cheaper sensors and devices for indicative citizen-based monitoring of respirable particulate matter. *Environ. Pollut.* **2015**, *206*, 696–704. [CrossRef] [PubMed]
28. Khan, A.U.; Khan, M.E.; Hasan, M.; Zakri, W.; Alhazmi, W.; Islam, T. An Efficient Wireless Sensor Network Based on the ESP-MESH Protocol for Indoor and Outdoor Air Quality Monitoring. *Sustainability* **2022**, *14*, 16630. [CrossRef]
29. Plantower. Available online: www.plantower.com (accessed on 9 February 2023).
30. Sensirion. Available online: www.sensirion.com (accessed on 9 February 2023).
31. Website Page of ARPA Puglia. Available online: www.arpa.puglia.it (accessed on 9 February 2023).
32. Website Page of ARPA Puglia Monitoring Data. Available online: http://old.arpa.puglia.it/web/guest/qariainq2 (accessed on 9 February 2023).
33. Zamora, M.L.; Rice, J.; Koehler, K. One year evaluation of three low-cost $PM_{2.5}$ monitors. *Atmos. Environ.* **2020**, *235*, 117615. [CrossRef] [PubMed]
34. SentinAir Project Repository. Available online: https://github.com/domenico-suriano/SentinAir (accessed on 9 February 2023).
35. Suriano, D. A portable air quality monitoring unit and a modular, flexible tool for on-field evaluation and calibration of low-cost gas sensors. *HardwareX* **2021**, *9*, e00198. [CrossRef] [PubMed]
36. Suriano, D. SentinAir system software: A flexible tool for data acquisition from heterogeneous sensors and devices. *SoftwareX* **2020**, *12*, 100589. [CrossRef]
37. Suriano, D.; Cassano, G.; Penza, M. Design and Development of a Flexible, Plug-and-Play, Cost-Effective Tool for on-Field Evaluation of Gas Sensors. *J. Sens.* **2020**, *2020*, 8812025. [CrossRef]
38. Raspberry. Available online: www.raspberrypi.com (accessed on 9 February 2023).
39. Abelectronics. Available online: https://www.abelectronics.co.uk (accessed on 9 February 2023).
40. Python. Available online: https://www.python.org (accessed on 9 February 2023).
41. Scikit. Available online: https://scikit-learn.org/stable/index.html (accessed on 9 February 2023).
42. Pedregosa, F.; Varoquaux, G.; Gramfort, A.; Michel, V.; Thirion, B.; Grisel, O.; Blondel, M.; Prettenhofer, P.; Weiss, R.; Dubourg, V.; et al. Scikit-learn: Machine Learning in Python. *JMLR* **2011**, *12*, 2825–2830.
43. Buitinck, L.; Louppe, G.; Blondel, M.; Pedregosa, F.; Mueller, A.; Grisel, O.; Niculae, V.; Prettenhofer, P.; Gramfort, A.; Grobler, J.; et al. API design for machine learning software: Experiences from the scikit-learn project. *arXiv* **2013**, arXiv:1309.0238v1.
44. Crilley, L.R.; Shaw, M.; Pound, R.; Kramer, L.J.; Price, R.; Young, S.; Lewis, A.C.; Pope, F.D. Evaluation of a low-cost optical particle counter (Alphasense OPC-N2) for ambient air monitoring. *Atmos. Meas. Tech.* **2018**, *11*, 709–720. [CrossRef]
45. Di Antonio, A.; Popoola, O.A.M.; Ouyang, B.; Saffell, J.; Jones, R.L. Developing a Relative Humidity Correction for Low-Cost Sensors Measuring Ambient Particulate Matter. *Sensors* **2018**, *18*, 2790. [CrossRef] [PubMed]